

# Enhanced Aromaticity of the Transition Structures for the Diels–Alder Reactions of Quinodimethanes: Evidence from *ab Initio* and DFT Computations

Mariappan Manoharan,<sup>†</sup> Frank De Proft, and Paul Geerlings\*

*Eenheid Algemene Chemie, Vrije Universiteit Brussel, Faculteit Wetenschappen, Pleinlaan 2, B-1050 Brussels, Belgium*

*pgeerlin@vub.ac.be*

*Received July 31, 2000*

The Diels–Alder reactions of various quinodimethanes with ethylene are studied by means of *ab initio* molecular orbital and density functional theory (DFT) to show the effect of aromaticity on the reaction path. The calculations reveal that these reactions are both kinetically and thermodynamically much more favored than the prototype butadiene–ethylene Diels–Alder reaction due to the aromatization process in the transition state (TS) and product. A progressive aromaticity gain is noticed during the reaction, and hence the partial  $\pi$ -delocalized peripheral diene ring function is coupled with the six-electron  $\sigma,\pi$ -delocalized cyclic unit resulting in an enhanced aromaticity of the TS. The magnetic criteria such as magnetic susceptibility exaltation and nucleus independent chemical shift provide definitive evidence for and fully support the aromatization process and the aromaticity of the TS. The extent of  $\sigma$ – $\pi$  delocalization and the bond make–break at the TS are consistent with each other, and this is strongly influenced by the adjacent  $\pi$ -aromatization process. Moreover, the aromaticity trends in the resulting TSs and products parallel the activation and reaction energies; the extent of aromatization increases with increasing reaction rate and exothermicity. This confirms that aromaticity is the driving factor governing cycloadditions involving quinodimethanes.

## 1. Introduction

The *in situ* generated *o*-quinodimethanes<sup>1</sup> are highly sensitive and powerful reactive intermediates used as dienes in Diels–Alder cycloadditions. Their importance in organic synthetic chemistry prompted the development of new kinds of carbo-<sup>2</sup> and heterocyclic<sup>3</sup> quinodimethanes used in the preparation of different natural products.<sup>1a</sup> These dienes are known to yield extremely stable cycloadducts owing to the aromatization of the resulting products; they belong to the category of masked dienes, in the sense that the reacting functions are fused to a ring in an *exo* fashion and can thus be referred to as ring-

fused or outer-outer ring dienes. Due to the changes in the diene functionality during the course of the reaction, the rest of the ring function becomes aromatic, and this effect reinforces the outcome of the reaction by sustaining a stable aromatic Diels–Alder adduct.

A general criterion which quantifies both aspects of aromatization in these reactions<sup>1–3</sup> has not been formulated yet and only a few theoretical studies<sup>4,5</sup> along this line are available. We therefore selected a set of Diels–Alder reactions involving various quinodimethanes (**1–9**) and ethylene (Figure 1) to quantify the aromaticity factors that drive the reactions through the computed energies and magnetic properties. On the other hand, the transition state (TS) of Diels–Alder<sup>6a</sup> and other pericyclic reactions<sup>6b</sup> was assumed to be a delocalized cyclic aromatic and this is authentically proven by the recent computational studies<sup>7</sup> based on the magnetic criteria. This leads to a new insight into the TSs of these quinodimethane reactions: *the usual six-electron cyclic delocalization ( $\sigma,\pi$ ) will be accompanied by the partial delocalization ( $\pi$ ) of the peripheral ring of diene during the*

<sup>†</sup> On leave of absence from School of Chemistry, University of Hyderabad, Hyderabad-500 046, India.

\* E-mail: pgeerlin@vub.ac.be.

(1) For a review see: (a) Klundt, I. *Chem. Rev.* **1970**, *70*, 471. (b) Quinkert, Stark, H. *Angew. Chem., Int. Ed. Engl.* **1983**, *22*, 637. (c) Wong, H. N. C.; Lau, K.-L.; Tam, K.-K. *Top. Curr. Chem.* **1986**, *133*, 85. (d) Charlton, J. L.; Alauddin, M. M. *Tetrahedron* **1987**, *43*, 2873. (e) Martin, M.; Seoane, C.; Hanack, M. *Org. Prepr. Prod. Int.* **1991**, *23*, 237. (f) Segura, J. L.; Martin, N. *Chem. Rev.* **1999**, *99*, 3199.

(2) (a) D'Andrea, S. V.; Freeman, J. P.; Szmuskovicz, J. *J. Org. Chem.* **1990**, *55*, 4356. (b) Rubin, Y.; Khan, S.; Freedberg, D. I.; Yerezain, C. *J. Am. Chem. Soc.* **1993**, *115*, 344. (c) Parakka, J. P.; Sadanandan, E. V.; Cava, M. P. *J. Org. Chem.* **1994**, *59*, 4308. (d) Nelik, P.; Gügel, A.; Walter, M.; Müllen, K. *J. Org. Chem.* **1995**, *60*, 3307.

(3) (a) Pindu, U.; Erfanian-Abdoust, H. *Chem. Rev.* **1989**, *89*, 1681. (b) Haber, M.; Pindur, U. *Tetrahedron* **1991**, *47*, 1925. (c) Tomé, A. C.; Cavaleiro, J. A. S.; Storr, R. C. *Tetrahedron Lett.* **1993**, *34*, 6639. (d) Chou, T.; Ko, C. *Tetrahedron* **1994**, *50*, 10721. (e) Carly, P. R.; Cappelle, S. L.; Compornolle, F.; Hoornaert, G. *J. Tetrahedron* **1996**, *52*, 11889. (f) Torres-García, G.; Luftmann, H.; Wolff, Mattay, J. *J. Org. Chem.* **1997**, *62*, 2752. (g) Fernandez U. M.; Illescas, B.; Martín, N.; Seoane, C.; Cruz, P.; Hoz, A.; Langa, F. *J. Org. Chem.* **1997**, *62*, 3705. (h) González, B.; Herrera, A.; Illescas, B.; Martín, N.; Martínez, R.; Moreno, F.; Sánchez, L.; Sánchez, A. *J. Org. Chem.* **1998**, *63*, 6807. (i) Martín, N.; Martínez-Grau, A.; Seoane, C.; Torres, M. *J. Org. Chem.* **1998**, *63*, 8074.

(4) Manoharan, M.; Venuvanalngam, P. *J. Phys. Org. Chem.* **1998**, *11*, 133.

(5) (a) Jursic, B. S. *J. Chem. Soc., Perkin Trans. 2* **1995**, 1217. (b) Chao, I.; Lu, H.; Chou, T. *J. Org. Chem.* **1997**, *62*, 7882. (c) Jursic, B. S. *Tetrahedron* **1997**, *53*, 13285.

(6) (a) Evans, M. G.; Warhurst, E. *Trans. Faraday Soc.* **1938**, *34*, 614. (b) Zimmerman, H. *Acc. Chem. Res.* **1971**, *4*, 272.

(7) (a) Herges, R.; Jiao, H.; Schleyer, P. v. R. *Angew. Chem., Int. Ed. Engl.* **1994**, *33*, 1376. (b) Jiao, H.; Schleyer, P. v. R. *Angew. Chem., Int. Ed. Engl.* **1995**, *34*, 334. (c) Jiao, H.; Schleyer, P. v. R. *J. Am. Chem. Soc.* **1995**, *117*, 11529. (d) Jiao, H.; Schleyer, P. v. R. *J. Phys. Org. Chem.* **1998**, *11*, 655. (e) Marao, I.; Cossio, F. P. *J. Org. Chem.* **1999**, *64*, 1868. (f) Cossio, F. P.; Marao, I.; Jiao, H.; Schleyer, P. v. R. *J. Am. Chem. Soc.* **1999**, *121*, 6737.

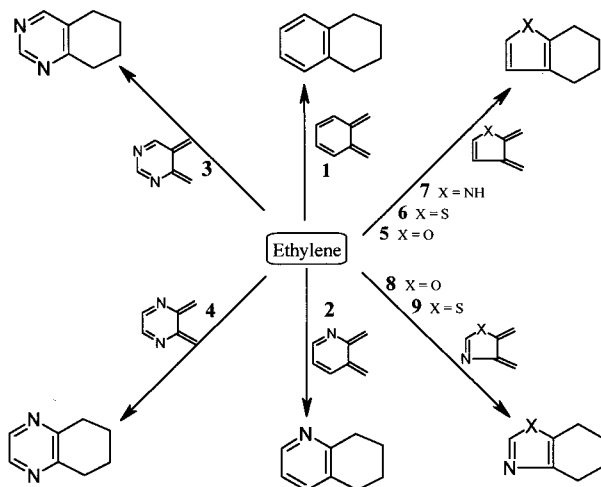


**Figure 1.** Series of quinodimethane reactions considered in this work.

formation of the TS resulting in an enhanced net aromaticity, increasing the reaction barrier relative to the prototype reaction. Moreover, the currently used magnetic susceptibility exaltation<sup>8</sup> (MSE) and Schleyer's nucleus independent chemical shift<sup>9</sup> (NICS) calculations are applied to explore the aromatic character of the systems involved in the reactions (Figure 1) and also to assess the aromaticity of the TSs. The aim of the present work is thus to investigate the dual-aromatic character of the TS involved in these reactions linking the reaction energetics with quantitative aromaticity indicators.

## 2. Theoretical and Computational Details

Computations for a series of quinodimethane reactions 1–9 (Figure 1) were performed with both *ab initio* and density functional theory (DFT) methods using Gaussian 94.<sup>10</sup> They all possess an extra aromatic ring fused to the cyclic "adduct" part. The reactants involve the derivatives of simple aromatic compounds viz. benzene, pyridine, pyrimidine, pyrazine, furan, thiophene, pyrrole, oxazole, and thiazole.<sup>1–3</sup> The stationary point geometries were fully optimized at the HF as well as B3LYP<sup>11</sup> levels with the 6-31G\* basis set<sup>12</sup> and were confirmed to be either minima or transition structures via a vibrational analysis. Single-point calculations were then carried out with both B3LYP/6-311+G\*\* and MP2/6-31+G\* levels on the B3LYP/6-31G\* geometries to evaluate the energetics. The magnetic susceptibilities involved in MSE, and the diamagnetic shieldings (NICS) were calculated respectively from CSGT<sup>13a</sup> and GIAO<sup>13a–c</sup> methods at the B3LYP/6-311+G\*\*//B3LYP/6-31G\* level. The methods chosen here are believed

to be quite adequate for the problem under study as witnessed by earlier reports.<sup>14</sup>

## 3. Results and Discussion

**(a) Transition State Geometry.** The reactions considered here all essentially follow a concerted mechanism.<sup>14</sup> Whereas the reactions involving 1 and 4 possess transition states (TS<sub>1</sub> and TS<sub>4</sub>) pointing to a synchronous mechanism due to the symmetry of the dienes, the other TSs (TS<sub>2</sub>–TS<sub>3</sub> and TS<sub>5</sub>–TS<sub>9</sub>) indicate an asynchronous mechanism due to the fact that these are all unsymmetrically functionalized dienes. As can be seen from the geometries (Figure 2), the C2–C3 bond length variations (numbering indicated in Figure 3) from reactant to TS and from TS to product fall in the range 0.035–0.061 and 0.046–0.067 Å, respectively. This  $\pi$ -bond formation is responsible for the fused diene ring to become partial and fully aromatic in the TS and product, respectively, thus favoring the bond-forming and -cleaving processes at the TS. The newly forming  $\sigma$  (C1–C6 and C4–C5) and  $\pi$  (C2–C3) bonds are noticeably much weaker and formed extremely fast whereas the cleaving  $\pi$ -bonds (C1–C2, C3–C4 and C5–C6) are slightly stronger and cleaved faster in the TSs (TS<sub>1</sub>–TS<sub>9</sub>) of different quinodimethane reactions (Figure 2) as compared to those found in the typical case (TS<sub>A</sub>). These bond criteria generalize the fact that the bond-forming ability surpasses the bond cleavage process due to aromatization when the former TSs are compared with the latter TS. Nevertheless, the extent of bond make–break at the TS is greater in the current TSs due to the partial aromatization attained at the TS and hence the "early" maturation of the TSs in relation to the prototype TS can be recognized from the above criteria.

The aromatic stabilization involved in the six-membered (benzene, pyridine, pyrimidine, and pyrazine) analogues of the TSs, TS<sub>1</sub>–TS<sub>4</sub>, should be more favorable for cycloaddition compared to the five-membered (furan, thiophene, pyrrole, oxazole, and thiazole) TS analogues (TS<sub>5</sub>–TS<sub>9</sub>) based on the aromaticity of the isolated systems involved<sup>8,9,15</sup> showing that the first set of systems is more aromatic than the latter set. Upon inspection of the length of the formed and cleaved bonds in the TS, the former TSs are indeed found to be earlier than the latter. The extent of aromatization in the TSs appears to be in agreement with the relative degree of bond formation and cleavage according to the trend in the reference aromaticity.<sup>8,9,15</sup> As can be seen, the larger aromatization corresponds to high degree of bond make–break at the TS.

**Aromaticity Enhancement in the TSs.** The  $\pi$ -bond alternation in the diene part of the TS is reduced from the reactant when the new  $\sigma$ -bonds are formed by disrupting the  $\pi$ -bond of the dienophile resulting in a rehybridization for all carbons. A six-electron  $\sigma,\pi$ -mixed

(8) (a) Dauben, J. H.; Wilson, J. D., Jr.; Laity, J. I. *J. Am. Chem. Soc.* **1968**, *90*, 1390. (b) Schleyer, P. v. R.; Jiao, H. *Pure Appl. Chem.* **1996**, *68*, 209. (c) Minkin, V. I.; Glukhovtsev, M. N.; Simkin, B. Y.; *Aromaticity and Antiaromaticity – Electronic and Structural Aspects*; John Wiley & Sons: New York, 1994.

(9) Schleyer, P. v. R.; Maerker, C.; Dransfield, Jiao, H.; van Eikema Hommes, N. J. R. *J. Am. Chem. Soc.* **1996**, *118*, 6317.

(10) Gaussian 94, Revision B.3, Frisch, M. J.; Trucks, G. H.; Schlegel, H. B.; Gill, P. M. W.; Johnson, B. G.; Robb, M. A.; Cheeseman, J. R.; Keith, T.; Petersson, G. A.; Montgomery, J. A.; Raghavachari, K.; Al-Laham, M. A.; Zakrzewski, V. G.; Ortiz, J. V.; Foresman, J. B.; Peng, C. Y.; Ayala, P. Y.; Chen, W.; Wong, M. W.; Andres, J. L.; Replogle, E. S.; Gomperts, R.; Martin, R. L.; Fox, D. J.; Binkley, J. S.; Defrees, D. J.; Baker, J.; Stewart, J. P.; Head-Gordon, M.; Gonzalez, C.; Pople, J. A. Gaussian, Inc.: Pittsburgh, PA, 1995.

(11) (a) Becke, A. D.; *J. Chem. Phys.* **1993**, *98*, 5648. (b) Stevens, P. J.; Devlin, F. J.; Chablowski, C. F.; Frisch, M. J. *J. Phys. Chem.* **1994**, *98*, 11623.

(12) Hehre, W. J.; Radom, L.; Schleyer, P. v. R.; Pople, J. *Ab initio Molecular Orbital Theory*; John Wiley & Sons: New York, 1986.

(13) (a) Cheeseman, J. R.; Trucks, G. W.; Keith, T. A.; Frisch, J. J. *J. Chem. Phys.* **1996**, *104*, 5497. (b) Wolinski, K.; Hilton, J. F.; Pulay, P. *J. Am. Chem. Soc.* **1990**, *112*, 8251. (c) Keith, T. A.; Bader, R. F. W. *Chem. Phys. Lett.* **1993**, *210*, 223.

(14) (a) Houk, K. N.; Li, Y.; Evanseck, J. D. *Angew. Chem., Int. Ed. Engl.* **1992**, *31*, 682. (b) Houk, K. N.; Gonzalez, J.; Li, Y. *Acc. Chem. Res.* **1995**, *28*, 81. (c) Wiest, O.; Houk, K. N. *Top. Curr. Chem.* **1996**, *183*, 1.

(15) (a) Katritzky, A. R.; Barczynski, P.; Masumarra, G.; Pisano, D.; Szafran, M. *J. Am. Chem. Soc.* **1989**, *111*, 7. (b) Bird, C. W. *Tetrahedron* **1996**, *29*, 9945. (c) Schleyer, P. v. R.; Freeman, P. K.; Jiao, H.; Goldfub, B. *Angew. Chem., Int. Ed. Engl.* **1995**, *34*, 337.

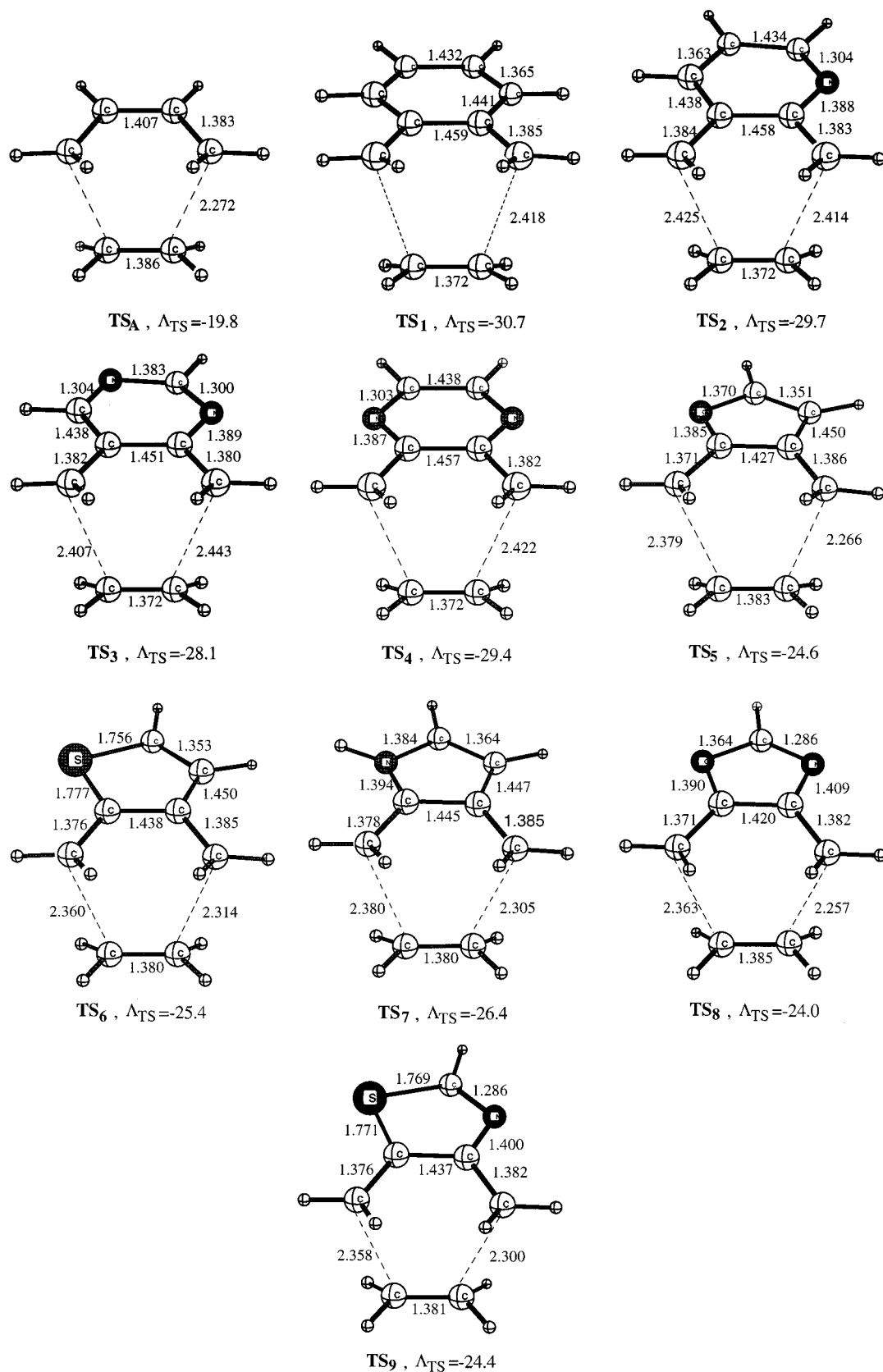


**Figure 2.** Computed B3LYP/6-31G\* TS geometries of various quinodimethane Diels–Alder additions to ethylene along with the forming and cleaving bonds (Å) and the MSE of TS (ppm cgs) obtained from B3LYP/6-311+G\*\* computations.

cyclic delocalized structure develops as suggested by Evans.<sup>6</sup> Consequently, the TS of prototype reaction (**TS<sub>A</sub>**) is predicted to be aromatic, as witnessed by the two magnetic criteria; the MSE ( $\Delta_{\text{TS}}$ ,  $-19.8$  ppm cgs) value as well as the NICS values at the center of two TS planes

( $-20.5$  and  $-24.4$  ppm) have large magnitudes.<sup>7a,d</sup> Moreover, these values are comparable to those obtained for benzene ( $\Delta_{\text{TS}}$ ,  $-13.7$ ; NICS,  $-10.2$ ). Apart from this, the TSs of the title reactions (**TS<sub>1</sub>**–**TS<sub>9</sub>**) indicate that partial  $\pi$ -delocalization arising from the aromatic stabilization

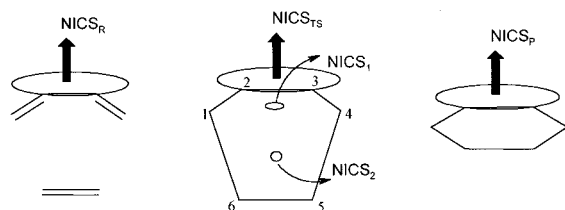
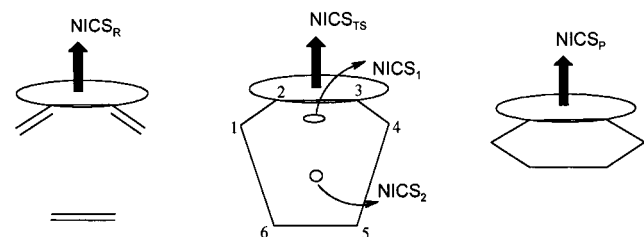


**Figure 3.** Schematic representation of the NICS calculations on reactant, TS, and products: the indices ( $\text{NICS}_R$ ,  $\text{NICS}_{TS}$ , and  $\text{NICS}_P$ ) representing the magnetic shielding calculated 1 Å above their respective peripheral ring centers. The in-plane aromaticity of the  $\text{TS}^{\text{9d-f}}$  is obtained from the  $\text{NICS}_1$  and  $\text{NICS}_2$  shielding at the center of their planes.

**Table 1. Results of NICS Calculations on Reactants, Transition States, and Products of the Different Quinodimethanes with Ethylene (B3LYP/6-311+G\*\*//B3LYP/6-31G\* level)<sup>a</sup>**



reaction	$\text{NICS}_R$	$\text{NICS}_{TS}$	$\text{NICS}_P$	$\text{NICS}_{iso}^b$	$\text{NICS}_1$	$\text{NICS}_2$
1	0.9	-5.5	-9.7	-10.2	-17.4	-22.0
2	0.5	-5.6	-9.6	-10.2	-16.8	-21.9
3	-0.1	-5.4	-9.7	-10.0	-17.7	-22.1
4	0.7	-5.3	-9.8	-10.2	-16.3	-21.8
5	-2.6	-6.1	-8.5	-9.9	-21.9	-24.1
6	-2.0	-5.9	-8.9	-10.2	-20.6	-23.2
7	-1.4	-6.7	-8.9	-10.1	-21.4	-23.4
8	-3.5	-6.2	-8.8	-9.6	-22.4	-24.7
9	-3.2	-6.6	-9.6	-10.9	-20.6	-23.5

<sup>a</sup> The different indices ( $\text{NICS}_R$ ,  $\text{NICS}_{TS}$ , and  $\text{NICS}_P$ ), also indicated in Figure 3, represent the magnetic shielding calculated 1 Å above their respective peripheral ring centers. The in-plane aromaticity of the TS is quantified by the  $\text{NICS}_1$  and  $\text{NICS}_2$  values in the respective plane centers. <sup>b</sup> NICS values calculated in the ring of the isolated aromatic systems (i.e., the rings peripheral to the diene function).

in the fused ring during the  $\pi$ -bond formation at the TS exists next to the normal cyclic  $\sigma, \pi$ -delocalization. These two different delocalizations enhance the aromaticity of the TS as compared to the prototype butadiene–ethylene reaction. The partial  $\pi$ -delocalized ring independently gains its aromaticity in all of the TSs by means of substantial diatropic shifts contributed by  $\text{NICS}_{TS}$  over the outside ring (Figure 3 and Table 1) ranging from -5.2 to -6.6 (Table 1) while the  $\sigma, \pi$ -delocalized cycle conserves alone its usual aromatic character at the same extent by securing large NICSs (-16.3 to -23.5 range) as found in the typical TS. Despite the fact that the aromaticity of the two individual rings of the concerned TSs can easily be understood from the different NICS indices (Table 1), the magnitude of the MSE of the  $\text{TS}^{16}$  ( $\Lambda_{TS}$  in Figure 2) provides further evidence for the net enhancement of the aromatic character of the TS. It is indeed confirmed by  $\Lambda_{TS}$  that the TSs ( $\text{TS}_1$ – $\text{TS}_9$ ) show an excess aromaticity caused by the  $\pi$ -delocalization of -4.2 to -10.9 ppm if one can consider the prototype TS ( $\text{TS}_A$ ) as the reference.

This is logically inferred from the  $\Lambda_{TS}$  values of the TSs (-24.0 to -30.7 ppm) under consideration as well as from the reference value (-19.8 ppm). The cyclic ( $\sigma$ - $\pi$ ) delocalization is completely lost in the product and this significantly reduces the aromaticity of the product as can be seen by comparing the  $\Lambda_{TS}$  (Figure 2) and  $\Lambda_P$ <sup>16</sup> (Table 1) values. Owing to the extra aromatic stabilization of the ring adjacent to the cyclic delocalized structure, the net aromaticity in all of the TSs is drastically increased, and this gives the clue for why these TSs are formed earlier over the typical case as shown by the bond criteria. This widely emphasizes the fact that the “earliness” of the TS is greatly achieved due to the enhanced aromaticity, and this would generally lead to a low barrier and a more exothermic reaction path.

It has to be remarked that  $\text{TS}_A$  and  $\text{TS}_1$  are benzene- and naphthalene-like, respectively. The aromatic stabilization energy of naphthalene is 12 kcal/mol larger than that of benzene,<sup>17</sup> in excellent agreement with the activation energy barrier difference between reaction A and 1 of 14.4 kcal/mol (B3LYP/6-311+G\*\*//B3LYP/6-31G\* level).

**(b) Degree of Aromatization in the Reaction Path.** The quinodimethanes (1–9) have different ring functions attached to a reactive diene framework, and these functions are nonaromatic due to the absence of a  $\pi$ -bond in the fused ring. This is clearly reflected in the NICS values ( $\text{NICS}_R$  in Table 1) found in the range of 0.9 to -3.5 ppm implying a small diamagnetic  $\pi$  ring current effect.<sup>7</sup> Their aromaticity is however successively increased during the TS and product formations through a  $\pi$ -bond fixation, and hence the corresponding NICS values presented in Table 1 ( $\text{NICS}_{TS}$  and  $\text{NICS}_P$ ) are found to be around -5.2 to -6.7 ppm for the TS and -8.5 to -9.7 ppm range for the product, respectively, which are reasonably higher than the reactant values. This happens because the  $\pi$ -bond growth (bond between carbon atoms 2 and 3 in Figure 3) increases from reactant to product via the TS, whereas the other  $\pi$ -bonds in the six- and five-membered rings remain unaltered. Moreover, the aromatization of the resulting TS and product is apparently of great importance for both the kinetic and thermodynamic aspects of the reaction, since that particular ring accounts for 50–65% and 85–97% aromaticity for TS and product, respectively (cf. the comparison of the NICS values of these rings in the TSs and products to the NICS of related isolated aromatic rings ( $\text{NICS}_{iso}$  in Table 1)).

**(c) Energetics vs MSE.** The aromatic functionalization in various quinodimethane reactions (1–9) enhances the speed of reaction compared to the prototype reaction (A) as revealed by the activation energies calculated at different levels (Table 2). This is evident from the fact that the TSs of these reactions ( $\text{TS}_1$ – $\text{TS}_9$ ) have two kinds of delocalizations resulting in an enhanced aromaticity with respect to  $\text{TS}_A$ . This effect remarkably reduces the reaction barriers. A huge difference in the barrier between the present reactions and the simplest case (i.e., the butadiene–ethylene reaction) can also be noticed. Subsequently, this aromatization process guides all of the reactions to the more exothermic paths through the “early” nature of the TSs shown by the bond and magnetic criteria; as a result, the exothermicity of the reaction is largely increased over the prototype case, in

(16) The magnetic susceptibility of the TS ( $\Lambda_{TS}$ ) and the product ( $\Lambda_P$ ) are calculated by considering the reactants as reference systems. See also ref 7.

(17) Tokitoh, N.; Okazaki, R.; Nagase, S.; Schleyer, P. v. R.; Jiao, H. *J. Am. Chem. Soc.* **1999**, *121*, 11336.

**Table 2.** Calculated Activation and Reaction Energies (kcal mol<sup>-1</sup>) Obtained from Various *ab Initio* and DFT Calculations, and MSE of the Product ( $\Delta_P$ , ppm cgs) for Different Quinodimethanes (1–9) and Prototype (A) Diels–Alder Reactions

reaction	$\Delta E^{\ddagger}$				$\Delta E_r$				$\Delta_P$
	I <sup>a</sup>	II <sup>b</sup>	III <sup>c</sup>	IV <sup>d</sup>	I	II	III	IV	
A	45.0	22.4	25.4	18.4	-42.9	-43.1	-35.7	-48.7	-4.9
1	29.6	8.5	11.0	1.9	-72.3	-70.9	-63.5	-82.6	-21.4
2	29.3	8.2	10.6	1.7	-73.1	-71.6	-64.6	-83.4	-20.8
3	28.8	7.7	10.2	1.9	-73.6	-71.9	-65.0	-83.2	-19.0
4	29.3	7.7	10.0	1.4	-73.2	-72.3	-65.8	-84.4	-21.0
5	38.7	15.6	18.4	8.4	-54.1	-54.7	-47.4	-66.2	-11.1
6	35.8	13.7	16.3	6.0	-57.4	-57.7	-50.7	-70.2	-14.5
7	36.3	13.8	16.5	5.8	-58.5	-58.3	-50.7	-71.3	-13.3
8	39.8	16.5	19.2	9.4	-52.1	-53.0	-46.0	-64.5	-10.3
9	36.2	14.0	16.6	6.3	-57.0	-57.2	-50.5	-69.8	-13.8

<sup>a</sup> (I) HF/6-31G\*/HF/6-31G\* level. <sup>b</sup> (II) B3LYP/6-31G\*\*/B3LYP/6-31G\* level. <sup>c</sup> (III) B3LYP/6-311+G\*\*/B3LYP/6-31G\* level. <sup>d</sup> (IV) MP2/6-31+G\*\*/B3LYP/6-31G\* level.

accordance with Hammond's postulate.<sup>18</sup> It can thus be concluded that both the kinetic and thermodynamic aspects of all quinodimethane–ethylene reactions are more favored than the typical butadiene–ethylene reaction, due to the strong influence of the aromatization of TS and product.

As also witnessed in ref 14, the activation barriers show rather large differences for the four theoretical levels used in this work. Upon comparison with the B3LYP/6-311+G\*\*/B3LYP/6-31G\*, the HF/6-31G\*/HF/6-31G\* barriers are in general too high, whereas the MP2/6-31+G\* ones are too low. However, the barrier trends, of importance in this work, remain more or less unaltered when the four levels of theory are compared.

With the aromatization process, the cycloadditions involving the six-membered fused dienes (1–4) form benzene-, pyridine-, pyrimidine-, and pyrazine-like TSs and products whereas the five-membered fused dienes (5–9) yield furan-, thiophene-, pyrrole-, oxazole-, and thiazole-type derivatives. The extent of aromatization in the former set of reactions set is predicted to be larger than that in the latter, because the aromaticity of the former TS and product derivatives are considerably higher than that of the latter as witnessed by the  $\Delta_{TS}$  (Figure 2) and  $\Delta_P$  (Table 1) values, respectively. The MSE values of the first four TSs and products ranging from -28 to -31 and -19 to -21 ppm, respectively, which is approximately -4 ppm higher than the latter cases (-24.0 to -26.4 and -11.1 to -14.5 ppm). This is in accordance with the relative aromaticity of these two kinds of isolated systems assessed by energetic and magnetic criteria.<sup>9,15</sup> In this context, the TSs (TS<sub>1</sub>–TS<sub>4</sub>) of the former reactions are expected to be formed earlier with lower barriers (Table 2) compared to the latter reactions. As anticipated, the high degree of aromatization in the product found for reactions 1–4 leads to the more exothermic reaction path relative to reactions 5–9 as can be seen from the reaction energies (Table 2). Calculations further indicate that the latter reactions are kinetically as well as thermodynamically less favorable than the former reactions due to the strained five-membered ring function involved in the reaction. Benzene is known to be slightly more aromatic than its aza (pyridine) and diaza (pyrimidine and pyrazine) derivatives,<sup>15</sup> and this aromaticity pattern is reproduced by the

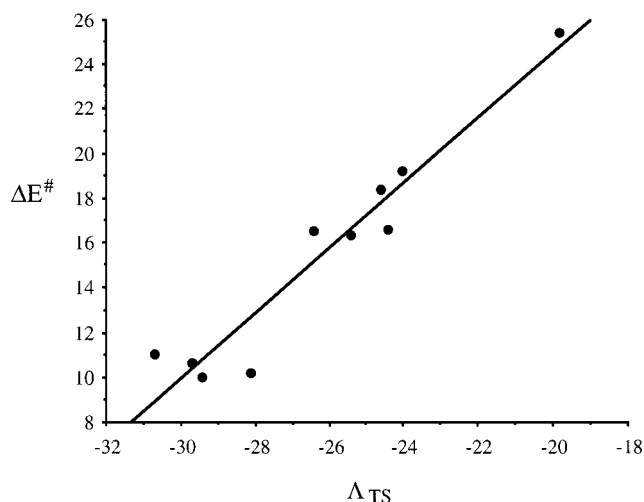


**Figure 4.** Correlation of the calculated activation energies  $\Delta E^{\ddagger}$  (kcal/mol) of the quinodimethane–ethylene reactions with the MSE value of the transition states ( $\Delta_{TS}$ ) (ppm cgs).

aromatized TSs and products of reactions 1–4, since the MSE ( $\Delta_{TS}$  and  $\Delta_P$ ) values of the benzene analogue presented in Figure 2 and Table 1 slightly exceeds those found in the other derivatives. However, the aromatic nature of these TSs and products are almost similar, and therefore, the TSs are formed mostly at the same speed. Accordingly, the kinetic and thermodynamic aspects of these reactions are also similar if one looks at the activation and reaction energies (Table 2). However, it should be remarked that reactions 2–4 have a slightly lower activation barrier and higher exothermicity than 1, although the degree of aromatization is smaller. This is probably due to the fact that the electron-donating ability toward the diene is slightly higher for these compounds which eventually overcomes the influence of aromaticity. Among the TS and product derivatives of furan, thiophene and pyrrole, the furan functionalization in reaction 5 is expected to be less favorable than the rest of the two processes (6 and 7), because the aromatized furan analogues of both TS and product are observed to be relatively less aromatic than the other two aromatized analogues as predicted by the basic systems.<sup>9,15</sup> Reaction 5 thus forms a “late” TS with high barrier that leads to a less exothermic path compared to that of 6 and 7. The extent of aromatization in the reactions 6 and 7 is nearly the same and therefore they have almost the same barrier and reaction energies, although thiophene is shown to be slightly more aromatic than pyrrole.<sup>9,15</sup> As shown by the aromaticity of oxazole and thioxazole,<sup>9,15</sup> the aromatization in the thioxazole-like TS and product is somewhat greater than the oxazole cases as witnessed by  $\Delta_{TS}$  (Figure 1) and  $\Delta_P$  (Table 1). Therefore, reaction 9 is faster and more exothermic than 8 as revealed by the activation and reaction energies (Table 2).

The genuine role of aromaticity in both the kinetic and thermodynamic aspects of these reactions is proved to be true as the correlation between the aromaticity of the TS ( $\Delta_{TS}$ ) and the barriers is found to be 92.2% while the aromaticity of the product ( $\Delta_P$ ) vs reaction correlation amounts to 97.2% as shown in Figures 4 and 5. Overall, the calculations establish the fact that aromaticity is the most prominent factor for the Diels–Alder reactions involving any quinodimethanes; the low barrier and more

(18) Hammond, G. S. *J. Am. Chem. Soc.* **1955**, *77*, 3.

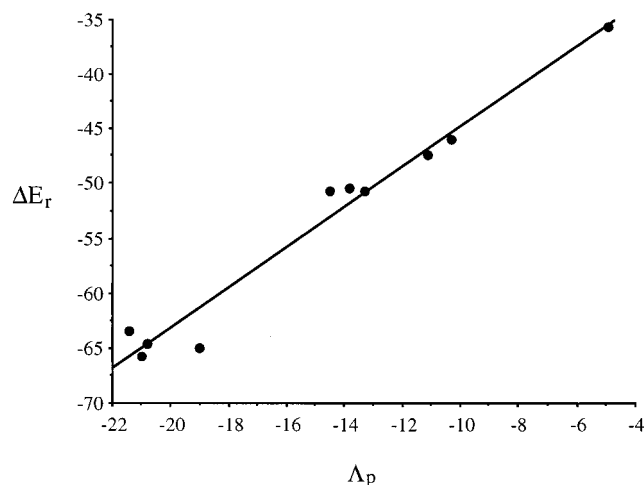


**Figure 5.** Correlation of the calculated reaction energies  $\Delta E_r$  (kcal/mol) of the quinodimethane–ethylene reactions with the MSE value of the products ( $\Lambda_p$ ) (ppm cgs).

exothermic reaction is dictated by the high degree of aromaticity.<sup>19</sup>

#### 4. Conclusions

From the computed results, it can be broadly concluded that all quinodimethane reactions are faster and more

exothermic than the prototype butadiene–ethylene reaction in view of the aromatization. The resulting aromatized products are formed via a concerted TS which consists of both a cyclic  $\sigma, \pi$ -mixed delocalization of the adduct unit as well as a partial  $\pi$ -delocalization of the fused diene ring; the presence of these coupled delocalizations tremendously enhances their aromaticity relative to the prototype butadiene–ethylene reaction, thus exhibiting a lower barrier. Magnetic criteria, such as the nucleus independent chemical shifts (NICS) and the magnetic susceptibility exaltation (MSE) provide strong support for the progress and enhancement of the aromaticity. Furthermore, the calculations confirm that the high degree of aromaticity in the TS and product is responsible for the low barrier and the exothermicity of the reaction.

The MSE predicts that the six-membered ring fused dienes gain more aromaticity in the TSs than the five-membered ring fused ones. Consequently, the former set of reactions are kinetically as well as thermodynamically more favorable than the latter cases as revealed by the activation and reaction energies.

**Acknowledgment.** F. De Proft and M. Manoharan acknowledge the Fund for Scientific Research Flanders–Belgium (F.W.O.) for a postdoctoral and visiting postdoctoral fellowship, respectively. P.G. acknowledges the Fund for Scientific Research Flanders–Belgium (F.W.O.) and the Free University of Brussels (V.U.B.) for continuous support to his group.

JO001156K

(19) (a) Manoharan, M.; De Proft, F.; Geerlings, P. *J. Chem. Soc., Perkin Trans. 2* **2000**, 1767. (b) Manoharan, M.; De Proft, F.; Geerlings, P. *J. Org. Chem.* **2000**, *65*, 6132.